

# A hybrid MC-HS model for 3D analysis of tunnelling under piled structures

Ahmed F. Zidan<sup>\*1</sup> and Osman M. Ramadan<sup>2,3a</sup>

<sup>1</sup>Department of Civil Engineering, Faculty of Engineering, Beni-Suef University, Salah Salem Street 62511 Beni-Suef, Egypt

<sup>2</sup>Structural Engineering Department, Faculty of Engineering, Cairo University, Giza, Egypt

<sup>3</sup>Higher Technological Institute (HTI), 10th of Ramadan City, Egypt

(Received June 9, 2016, Revised September 21, 2017, Accepted September 25, 2017)

**Abstract.** In this paper, a comparative study of the effects of soil modelling on the interaction between tunnelling in soft soil and adjacent piled structure is presented. Several three-dimensional finite element analyses are performed to study the deformation of pile caps and piles as well as tunnel internal forces during the construction of an underground tunnel. The soil is modelled by two material models: the simple, yet approximate Mohr Coulomb (MC) yield criterion; and the complex, but reasonable hardening soil (HS) model with hyperbolic relation between stress and strain. For the former model, two different values of the soil stiffness modulus ( $E_{50}$  or  $E_{ur}$ ) as well as two profiles of stiffness variation with depth (constant and linearly increasing) were used in attempts to improve its prediction. As these four attempts did not succeed, a hybrid representation in which the hardening soil is used for soil located at the highly-strained zones while the Mohr Coulomb model is utilized elsewhere was investigated. This hybrid representation, which is a compromise between rigorous and simple solutions yielded results that compare well with those of the hardening soil model. The compared results include pile cap movements, pile deformation, and tunnel internal forces. Problem symmetry is utilized and, therefore, one symmetric half of the soil medium, the tunnel boring machine, the face pressure, the final tunnel lining, the pile caps, and the piles are modelled in several construction phases.

**Keywords:** tunnelling; soil-structure interaction; piled structure; strain-hardening; finite element; three-dimensional analysis

## 1. Introduction

Analysing the structure-foundation-soil interaction during tunnelling operation in a single coupled analysis is cumbersome. Realistic analysis of such systems can only be done using full, three-dimensional models that properly simulate the presence of existing structure, its foundation, appropriate material behaviour, and the tunnelling operation (Augarde *et al.* 1995, Chen *et al.* 1999 among others).

In general, numerical modelling contributed greatly in understanding the performance of shield tunnelling (Katzenbach and Breth 1981, Clough and Leca 1989, Addenbrooke 1996). Previous works investigated the effect of several factors that affect the tunnel soil pile interaction (Poulos 1979, Lee *et al.* 1992, Loganathan and Poulos 1998, Chen *et al.* 2000, Loganathan *et al.* 2000, Loganathan *et al.* 2001, Lee and Ng 2005, Pang 2006, Lee and Chiang 2007, Cheng *et al.* 2007, Yang *et al.* 2011, Linlong *et al.* 2012, Lee 2013, Ng *et al.* 2013, Zidan and Ramadan 2016, 2015).

Soil-structure interaction research studies attempt to simulate the behaviour of soil as it occurs in the field. To this end, few constitutive models are available: elastic,

elasto-plastic (e.g., Mohr-Coulomb), hardening soil, etc. (Zidan 2012, Ardakani *et al.* 2014, Mohammad and Tavakoli 2014, Moradi and Abbasnejad 2015). Obviously, the accuracy of soil-structure interaction simulations is controlled by the adopted soil stress-strain relationship and the correctness of the assumed numeric values for the model parameters. This statement is further elaborated below.

Samuel *et al.* (2013) compared the performance of braced excavation predicted by both the Mohr Coulomb (MC), and hardening soil (HS) constitutive models to the observed in-situ diaphragm wall deflections. According to their results, the HS model provided a competent result in comparison to observed diaphragm deflections, but the MC model significantly underestimated the diaphragm wall deflections.

A similar outcome was reported by Kahlström (2013) who performed a comparison of the MC and the HS material models of Plaxis-2D in estimating the primary consolidation behaviour of soft clay. His results indicated that performing design with the MC material model is inadequate while the most accurate results, when compared to actual survey measurements, were achieved when computing with the soft soil material model. Furthermore, in their study of tunnel excavation in weak rocks, Dong and Anagnostou (2013) stated that the MC yield criterion fails to map the non-linear stress-strain behaviour and the stress dependency of stiffness observed in triaxial testing on typical weak tectonized rocks such as kakirites. Besides, they reported that a modified HS model predicts the

\*Corresponding author, Associate Professor

E-mail: [ahmedzidan@eng.bsu.edu.eg](mailto:ahmedzidan@eng.bsu.edu.eg)

<sup>a</sup>Dean

E-mail: [osman-ramadan@eng.cu.edu.eg](mailto:osman-ramadan@eng.cu.edu.eg)



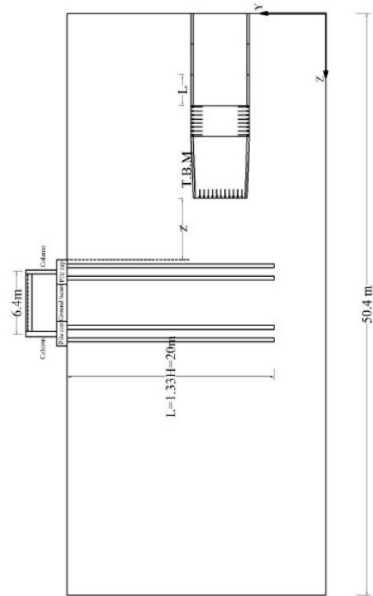


Fig. 3 Model geometry-longitudinal section



Fig. 4 The phase modelling in the phased excavation procedure (Plaxis manual)

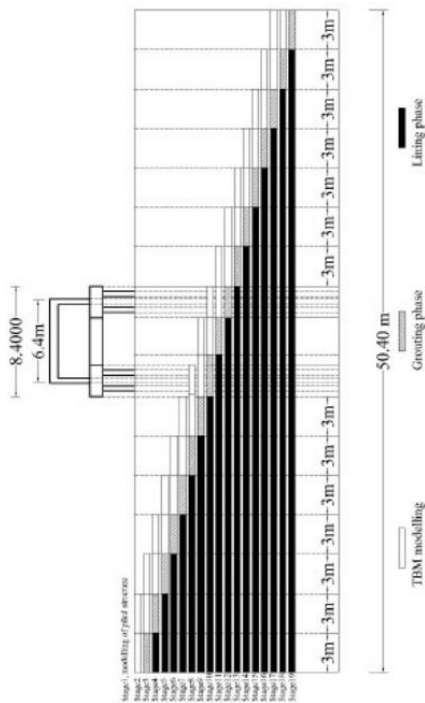


Fig. 5 Stages of tunnelling process

## 2. Numerical modelling

Numerical simulations are performed by means of the finite element program plaxis 3d tunnel (Brinkgreve and

Vermeer 2000). Data and analysis assumptions follow Zidan and Ramadan (2015), and are briefly summarized below for the sake of completeness. Due to symmetry of the analysed problem, only one half of the tunnel-soil-structure system is analysed. Analysis of the tunnelling-structure interaction problem is performed in two stages. The first stage determines the initial stresses in the soil mass and is performed in drained condition prior to the tunnel construction. It is performed considering the self-weight of both the soil and the structure. In the second stage, the analysis is performed under undrained condition. The displacements are reset to zero before starting of the tunnel installation to ensure that all deformations referred to hereafter are only a result of the tunnel construction.

The soil media is modelled using 15-node triangular prism elements and the initial effective stress is generated by means of the  $k_0$  procedure. Table 1 lists the adopted numerical values for the soil material model parameters. These values agree with the results of triaxial tests performed at Cairo University’s soil laboratory for several clayey soil sites in Egypt. In plaxis 3d tunnel program, the undrained analysis is modelled by effective stress analysis using effective parameters. It follows Terzaghi’s principal in which the total stress  $\sigma$  is given by

$$\sigma_{xx} = \sigma'_{xx} + \sigma_w, \sigma_{yy} = \sigma'_{yy} + \sigma_w, \sigma_{zz} = \sigma'_{zz} + \sigma_w, \sigma_{xy} = \sigma'_{xy}, \sigma_{yz} = \sigma'_{yz}, \sigma_{zx} = \sigma'_{zx} \quad (1)$$

where  $(\sigma_{ii} \text{ \& } \sigma'_{ii})$  and  $(\sigma_{ij} \text{ \& } \sigma'_{ij})$  are total and effective axial stresses and shear stresses, respectively, while  $\sigma_w$  is the pore water pressure. The above relations realize the fact that water does not sustain any shear stresses. In plaxis, the undrained behaviour is determined using the input effective model parameters. For more details on the soil material model, soil parameters, and undrained analysis, the reader may refer to plaxis manual.

By mean of 15-node volume elements, the tunnel lining, square piles, pile caps, beams, columns and slabs are assigned with specific weight  $\gamma=25 \text{ kN/m}^3$ , Young’s modulus  $E=2 \times 10^7 \text{ kN/m}^2$ , and Poisson’s ratio  $\nu=0.2$ . The tunnel geometry are given by: diameter  $D=5 \text{ m}$ , lining thickness  $t=0.35 \text{ m}$  and depth below ground surface  $H=3D$ . The model dimension and the structure geometry under consideration are presented in Figs. 1-3.

Referring to Fig. 3, the position of piled structure with regard to the tunnel is defined as:

$z^*$  =distance from tunnel face to the front edge of pile cap,

$L_{in}$  =tunnel face progress (distance) in each stage,

$y_p$  =distance from bottom of pile cap to any point on the pile length.

$L$  =length of pile.

As shown in the Fig. 2, each pile cap contains four piles. Two piles (P1 and P2) are selected to discuss the behaviour of other piles in the group. For the assumed super-structure, each pile carries 91 kN. The mesh presented in Fig. 5, which includes 8550 elements and 42970 nodes, is used for finite element analyses. The lateral boundaries of the model are located at a distance of  $5D$  (25 m) from the tunnel centre (see Fig. 1). Due to the huge number of elements and nodes in the current 3D model, a refined mesh is adopted around the tunnel and piles while a coarse mesh is adopted far away from the highly-strained area. In order to simulate the

progressive removal of elements, each construction segment ( $L_{in}$ ) is simulated by three stages. These three stages are: soil removal by the tunnelling boring machine (TBM); grouting; and final lining (Fig. 4). The analysis is done in 19 stages. In the first stage, the model is analysed under the effect of piled structure prior to the tunnelling process. The remaining 18 stages simulate the segmental construction of the tunnel (pouring, grouting, and lining) as shown in Fig. 5.

### 3. Types of conducted analyses

Table 2 shows the types of analyses conducted in this study. The system is first analyzed using the more reasonable hardening soil (HS) model, whose results are considered as the reference for other models. Then, the system analysis is repeated four times using different Mohr-Coulomb models (MC-1 to MC-4). These four MC models result from the permutation in the adopted Young's modulus ( $E_{50}$  or  $E_{ur}$ ) and the assumed profile of stiffness variation with depth (constant or linearly increasing). Finally, two hybrid simulations in which the HS model is used for soil located at the highly-strained zones and the MC model is utilized elsewhere are proposed and investigated. These hybrid or Modified Mohr-Column representations (MMC-1 and MMC-2) adopt  $E_{50}$  and differ only in the soil stiffness profile (constant for MMC-1 and linearly increasing for MMC-2).

Models MC-2 and MC-4 are represented through the option in plaxis that specifies a stiffness that varies linearly with depth. Two inputs are needed: a reference stiffness  $E_{ref}$  at a reference depth  $y_{ref}$ , and a rate of increment in stiffness per unit depth  $E_{inc}$ . At the reference confining pressure  $p_{ref}=100$  kPa, the same values as used for  $E_{50}^{ref}$  and  $E_{ur}^{ref}$  in the HS model are assigned to the MC-2 and MC-4 models, respectively. Table 3 shows the reference values and the stiffness increments for the cases of MC-2 and MC-4.

As will be shown later herein, the performance of all Mohr Coulomb (MC) models was not satisfactory in comparison with the reference HS model. Consequently, two hybrid models (MMC-1 and MMC-2) were proposed. In these models, the more accurate HS model is utilized in the high strained zones while the less accurate MC model is used in the less-strained zones. In this way, we could: (1) decrease computational time without sacrificing a great deal in the accuracy of results; and (2) reduce the amount of soil tests in the less-strained zones to those needed to determine the MC parameters only. Thus, compared to the HS model, the MMC models result in savings in both computational time and soil exploration costs.

Different scenarios may be suggested for selecting the high- and low-strained zones. Based on results of the HS model, the simple, yet efficient selection scenario shown in Fig. 6(a) is adopted. In Fig. 6(a), the soil elements within the foot prints of the superstructure, its foundation, and the tunnel are assigned with the HS model while the rest volume of soil is modelled using MC. This simple selection scenario keeps the hybrid model attractive for practicing engineers. Nevertheless, more efficient scenarios could be proposed based on refined criteria (e.g., considering a specific value of strain ratio to failure strain as a threshold). Such scenarios could lead to minimum computational time,

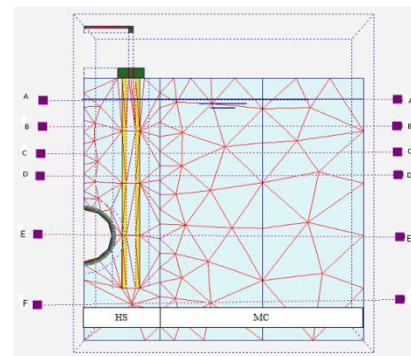
Table 2 Types of analyses

Analysis type	Analysis ID
Hardening-soil model.	HS
Mohr-Coulomb with $E_{50}$ constant with depth.	MC-1
Mohr-Coulomb with $E_{50}$ linearly increasing.	MC-2
Mohr-Coulomb with $E_{ur}$ constant with depth.	MC-3
Mohr-Coulomb with $E_{ur}$ linearly increasing.	MC-4
Modified Mohr-Coulomb with $E_{50}$ constant with depth (Hardening-soil model is used in highly-stressed zone).	MMC-1
Modified Mohr-Coulomb with $E_{50}$ linearly increasing with depth (Hardening-soil model is used in highly-stressed zone).	MMC-2

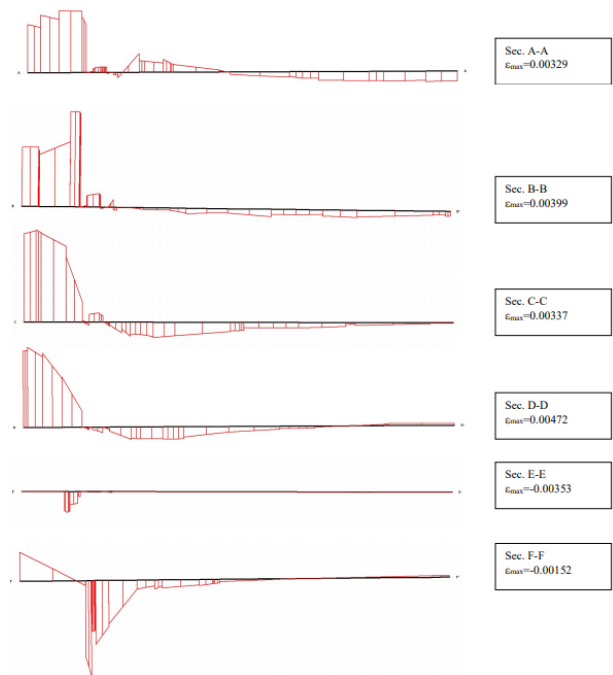
Table 3 Reference stiffness values for models MC-2 and MC-4

Analysis type	$E_{ref}$ (kPa)	$y_{ref}$ (m)*	$E_{inc}$ (kPa)
MC-2	527	2	83
MC-4	1317	2	209

\* $E_{ref}$  is assigned above  $y_{ref}$ , while below  $y_{ref}$  the stiffness is given by,  $E = E_{ref} + (y_{ref} - y)E_{inc}$



(a) Selecting zones with HS and MC soil models for the hybrid analyses: MMC-1 and MMC-2



(b) Strain distribution obtained from the HS model analysis for the steady state condition

Fig. 6 Selecting zones and Strain distribution obtained

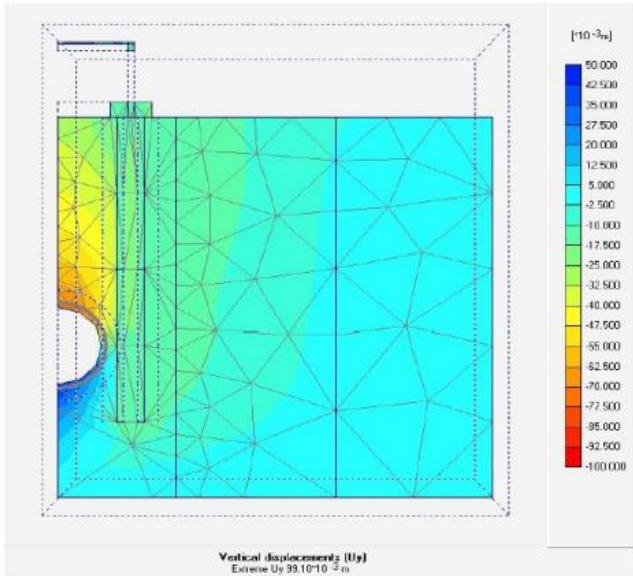


Fig. 7 Distribution of vertical displacement beneath the piled structure obtained from the HS model analysis for the steady state condition

but may render the analysis less-attractive or impractical.

To justify the simple scenario suggested for selecting the high- and low-strained zones, various horizontal sections along the width of model are selected as shown in Fig. 6(a). Fig. 6(b) shows the strain distribution at the horizontal sections (or planes) identified in Fig. 6(a) as obtained from the HS model analysis for the steady state condition. It is evident from Fig. 6(b) that the soil model assignment (HS/MC) shown in Fig. 6(a) is reasonable since the strain values in the soil mass represented by the MC are sufficiently small. This argument is further supported by the distribution of vertical displacement presented in Fig. 7 which reasonably small displacement values in the domain modelled using the MC soil material model in the proposed MMC models.

#### 4. Effect of tunnelling on soil deformation

Figs. 8(a)-8(c) present the displacements of ground surface for the steady state condition (i.e., after tunnelling is completed) in the transverse ( $u_x$ ), vertical ( $u_y$ ), and longitudinal ( $u_z$ ) directions, respectively, for the seven models described in Table 2. The effect of the super-structure presence on the ground surface deformations in the vicinity of the structure foundation is obvious from these figures. Besides, noticeable changes among results of different constitutive models are evident. Fig. 8(a) shows that the structure presence almost eliminates the transverse displacement in its vicinity. It is seen from Fig. 8(a) that the transverse displacement ( $u_x$ ) is fairly predicted by all models at structure foundation, but all MC models fail to produce accurate values away of the structure zone. The error in  $u_x$  associated with the use of MC constitutive relation (models MC-1 to MC-4) ranges from 30% to 80%. However, the proposed MMC models gave good estimates of  $u_x$  with less than 10% difference.

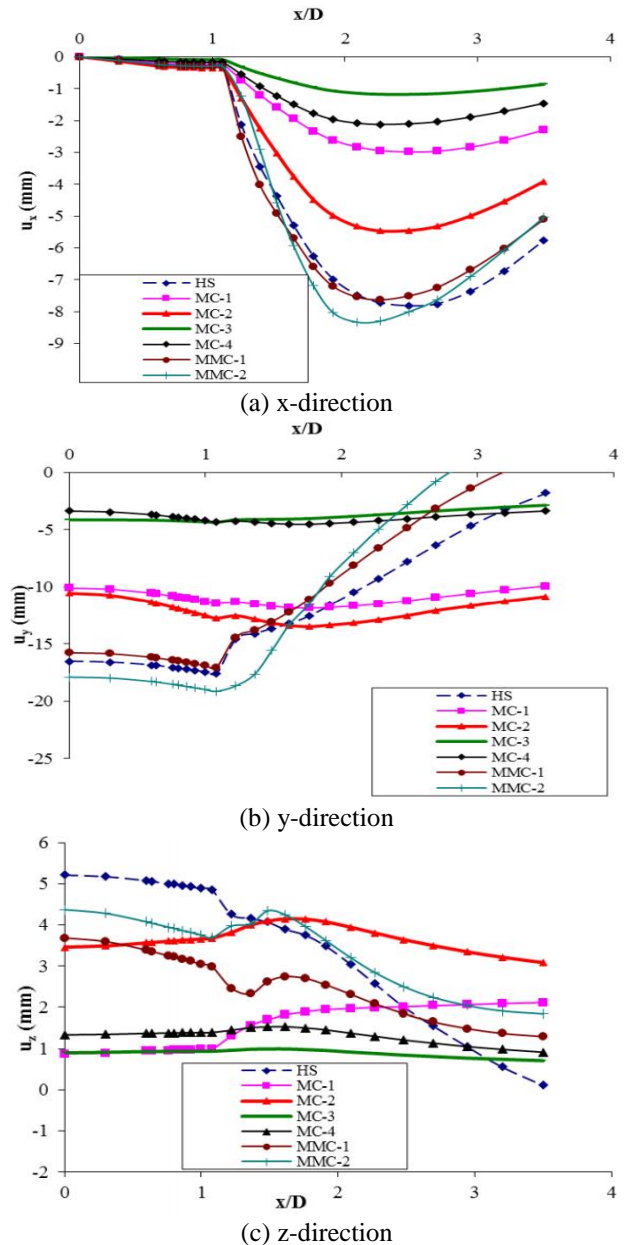


Fig. 8 Ground surface displacements after tunnelling

It is clear from Fig. 8(b) that the correct settlement profile  $u_y$  (at ground surface) obtained using the HS model has a flat shape in the vicinity of the structure foundation, followed by a sudden reduction at the pile cap outer edge, and decreases monotonically afterwards. Such behaviour could not be predicted by the various MC models (MC-1 to MC-4), but is fairly estimated by the proposed modified models (MC-1 and MC-2). Finally, Fig. 8(c) indicates that the behaviour of the various approximate models in predicting the surface displacement in tunnel longitudinal direction  $u_z$  is similar to their performance in predicting  $u_x$  and  $u_y$ . It is found that the type of soil modelling adopted in the analysis has a great effect on soil displacements both in value and distribution. The MC models fail to give reliable estimates, but the proposed modified models (MMC-1 and MMC-2) yielded reasonable approximation to the HS model results.

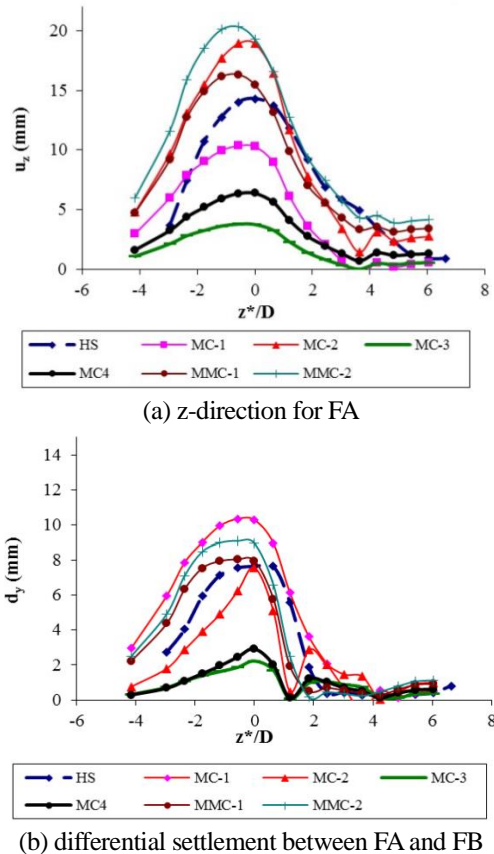


Fig. 9 Effect of soil modelling on the pile cap displacements during tunnelling

## 5. Effect of tunnelling on pile caps

Fig. 9(a) and 9(b) show variation of the longitudinal displacement ( $u_z$ ) of pile cap (FA) and the differential settlement ( $d_y$ ) between pile caps FA and FB, respectively, due to tunnel construction progress for the seven studied constitutive models. The lateral displacement ( $u_x$ ) under structure foundation is not shown as it is very small due to having the tunnel axis at the centre of the building in this study. Both  $u_z$  and  $d_y$  increase as the tunnel face approaches the pile cap and reach their maxima when the tunnel face crosses the pile cap and they decrease monotonically afterwards. Fig. 9(a)-9(b) highlight the significant effect of soil modelling on the pile cap displacement in z and y directions. For example, the maximum longitudinal displacement ( $u_z$ ) varies from 3mm to 19 mm while the maximum differential settlement ( $d_y$ ) changes from 2 to 11 mm due to various soil material models. The two MC models with  $E_{ur}$  (MC-3 & MC-4) give very poor results (about 25% of the results from the reference HS model). Besides, predictions obtained using MC models with  $E_{50}$  (MC-1 & MC-2) are either too-high or too-low compared to the reference HS model results. Finally, the best results are obtained using the proposed hybrid analysis with (MMC-2 model) where the difference from the HS model is less than 20% and 10% for  $u_z$  and  $d_y$ , respectively. Again, the results obtained using constant stiffness profile are generally better than those obtained assuming the stiffness (represented by either  $E_{ur}$  or  $E_{50}$ ) to increase linearly with depth.

## 6. Effect of tunnelling on piles

### 6.1 General behaviour of piles response

Now, we look at the deformation of piles due to tunnel construction as predicted by the various soil models. Figs. 10 and 11 present the pile deformation in the “transverse” XY plane ( $u_x$ ) for piles P1 and P2, respectively, at various stages of tunnel construction defined by the distance from tunnel face to the axis of pile,  $z_p$ . In general, Figs. 10 and 11 show that when the tunnel face is approaching the pile, the pile transverse deflection ( $u_x$ ) increases as the tunnelling operation advances and that the maximum value of  $u_x$  occurs in the middle third of the pile. Moreover, the value of ( $u_x$ ) increases with depth until its maximum value (at a depth of about 0.6 times L), then  $u_x$  decreases significantly with depth. After the tunnel face passes the pile location, the transverse deflection in the pile middle third decreases with the progress of tunnel construction and the maximum value shifts position to the pile tip. The piles deflect in double- or triple-curvature during tunnelling and the piles curvature continues to increase even after the tunnel face passes by the piles location. Therefore, higher internal forces develop in the piles after the tunnelling operation passes the structure location.

The distribution of the pile deflection in direction of the tunnel longitudinal axis (i.e.,  $u_z$ ) for piles P1 and P2 are displayed in Figs. 12 and 13. For the more accurate HS model, as the tunnel face progresses towards the structure, ( $u_z$ ) increases and has its highest value at pile heads. However, after tunnelling operation passes the pile location, values of  $u_z$  at pile heads decrease while the values at pile tips increase with the progress in tunnelling away of the structure. At the end of tunnel construction, the deflections at pile tips are higher than those at pile heads. Comparing Figs. 10 and 11 to Figs. 12 and 13 shows that while the pile deflections along the tunnel longitudinal axis ( $u_z$ ) are higher than the transverse ones ( $u_x$ ), the curvatures- and consequently the bending moments and shear forces- are higher in the transverse direction (i.e., in the XY plane). For more details on general piles behaviour including pile internal forces, refer to Zidan and Ramadan (2015).

### 6.2 Effect of soil modelling on piles flexural response

It is obvious from Figs. 10-13 that when the soil media is modelled by the MC criterion (MC-1 to MC-4), the pile deformation is grossly exaggerated compared to that obtained by the HS constitutive model. Errors in MC prediction of pile deformation as large as 200% are observed with similarly-high errors in pile curvature (bending moments). However, a much better predictions of pile deformation could be obtained using the proposed hybrid models (MMC-1 & MMC-2). While the pile deflections predicted by MMC-1 and MMC-2 show a moderate agreement with the results obtained by the HS model, the pile curvatures, and consequently the pile bending moments, reveal a much better agreement. Besides, the hybrid model with  $E_{50}$  constant with depth (MMC-1) gives results that are generally closer to the HS results than does the hybrid model with  $E_{50}$  linearly increasing with depth.

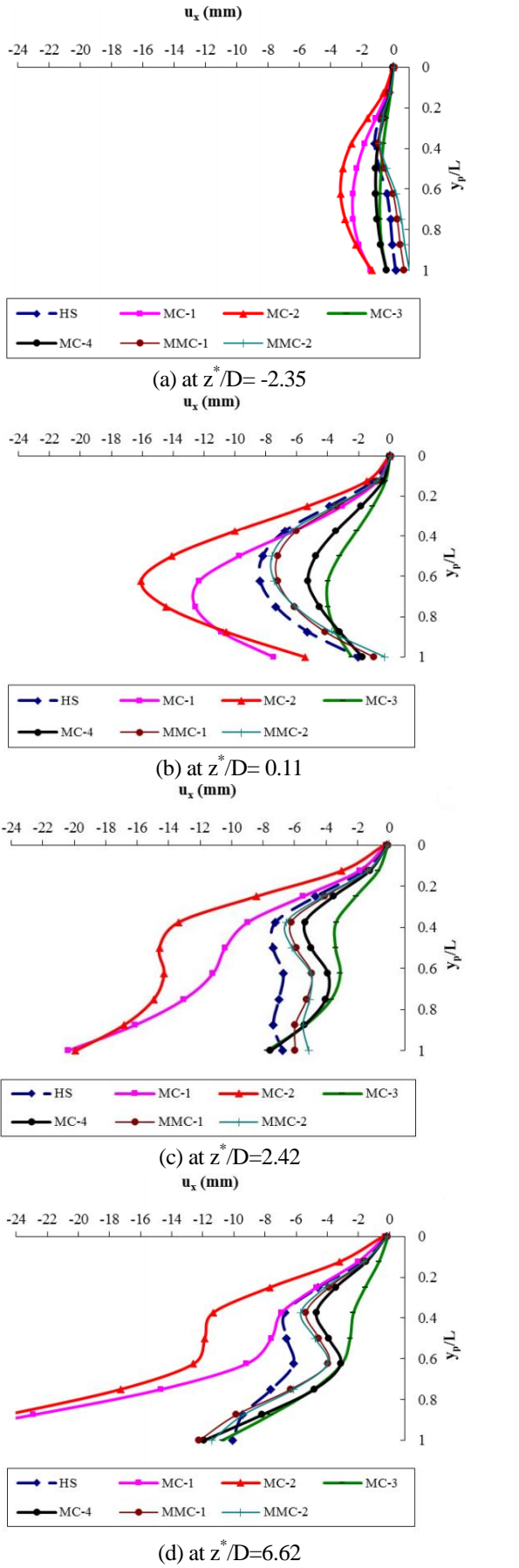


Fig. 10 Deformation of pile (P1) in x-direction during tunnelling

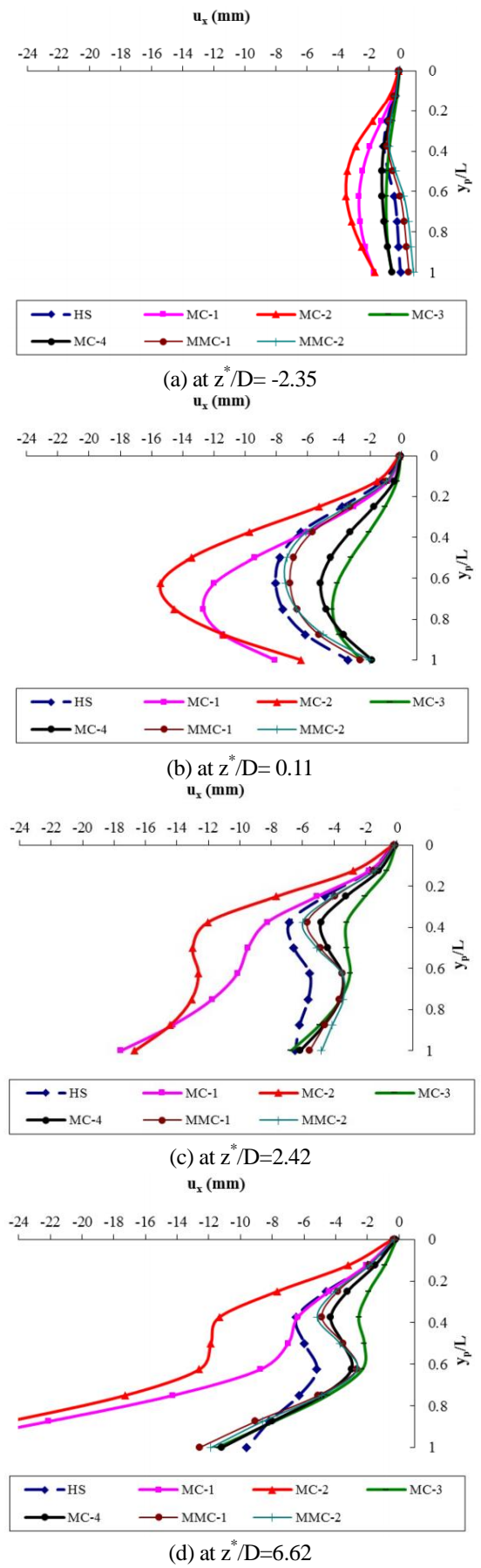
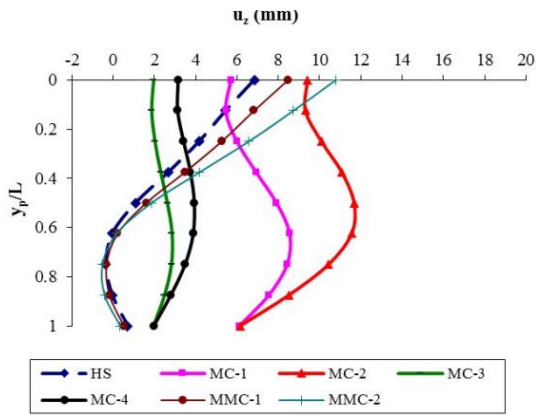
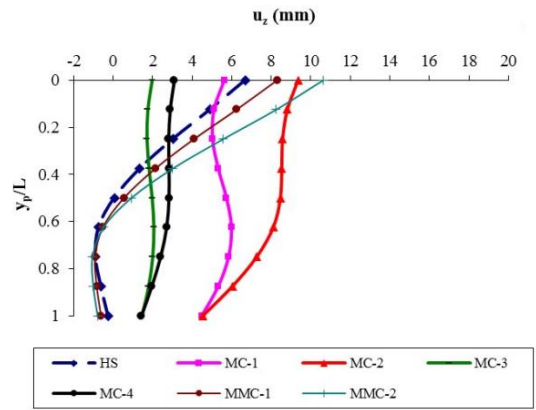


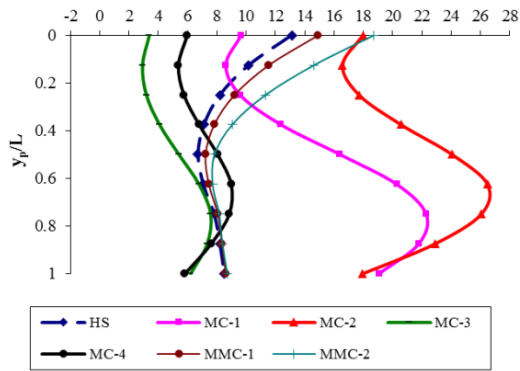
Fig. 11 Deformation of pile (P2) in x-direction during tunnelling



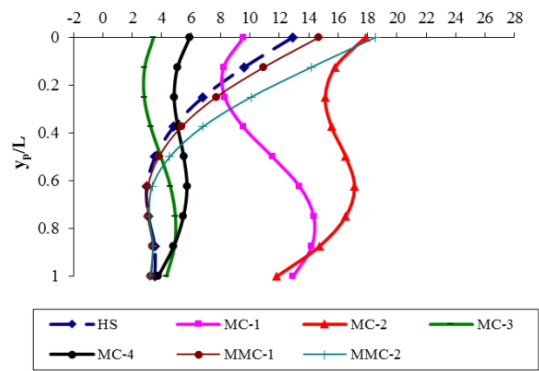
(a) at  $z^*/D = -2.35$



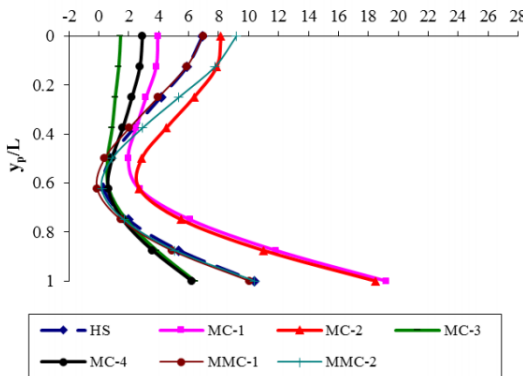
(a) at  $z^*/D = -2.35$



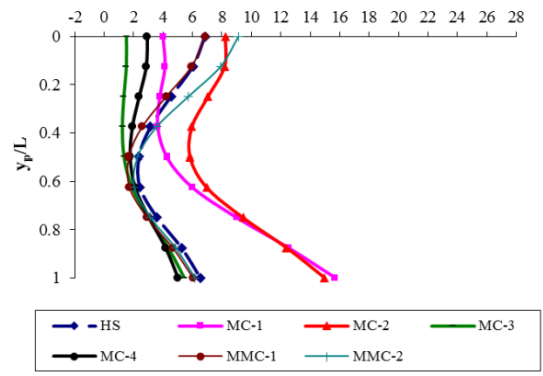
(b) at  $z^*/D = 0.11$



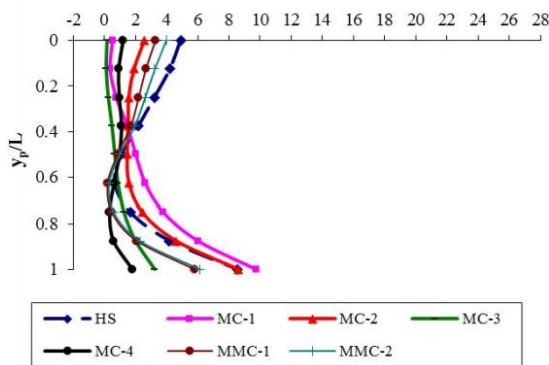
(b) at  $z^*/D = 0.11$



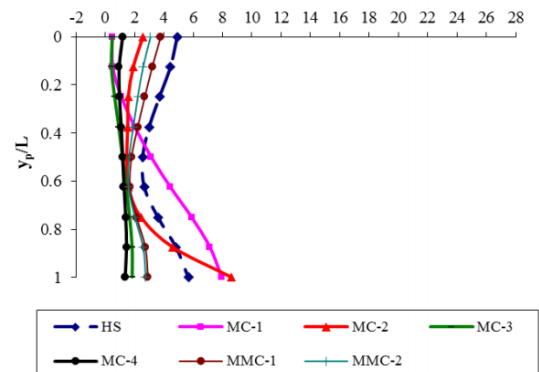
(c) at  $z^*/D = 2.42$



(c) at  $z^*/D = 2.42$



(d) at  $z^*/D = 6.62$



(d) at  $z^*/D = 6.62$

Fig. 12 Deformation of pile (P1) in z-direction during tunnelling

Fig. 13 Deformation of pile (P2) in z-direction during tunnelling

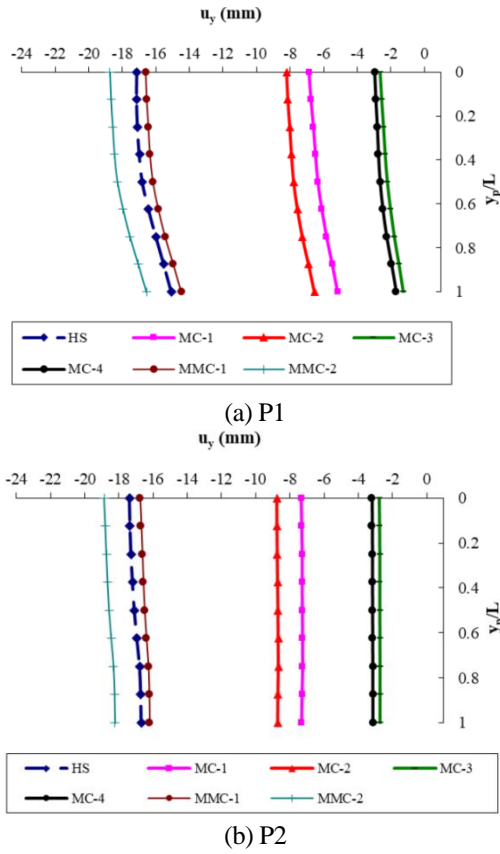


Fig. 14 Steady-state axial deformation of piles (displacement in y-direction)

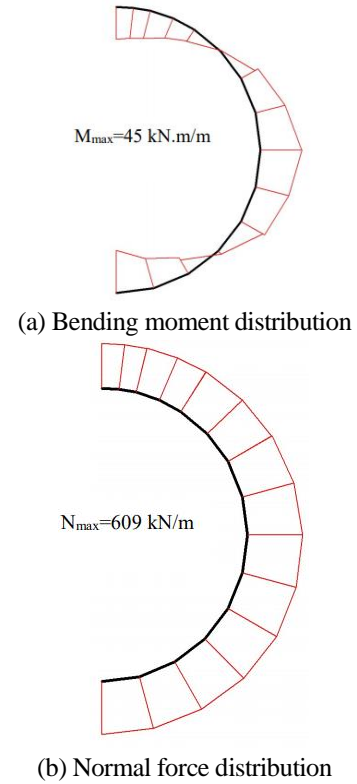


Fig. 16 Steady-state distributions of internal forces in tunnel lining shown for the case of HS model

### 6.3 Effect of soil modelling on pile axial forces

The construction of tunnelling alters the soil vertical displacements (settlement) beneath the piled structure. This consequently affects the axial response of piles. Fig. 14(a) and 14(b) present the steady-state axial response (i.e., vertical displacement distribution) of piles P1 and P2, respectively, obtained from the eight considered soil models. Both figures show that the MC models fail to match the HS model results, while the two MMC models give results that fairly compare with the HS results. Thus, the rest of this section focuses on the results of the HS and the MMC-1 models only.

The changes in axial deformation due to tunnelling along pile length indicate that tunnel construction produces additional axial loads in piles. These additional axial loads are presented in Figs. 15(a) and 15(b) at two construction stages: tunnelling directly under the structure ( $z^*/D=0.11$ ); and end of tunnelling ( $z^*/D=6.62$ ) for piles P1 and P2, respectively. Fig. 15(a) shows that high compressive force ( $\approx 350\text{kN}$ ) develops at the tip of pile P1, which is the closer to the tunnel, at  $z^*/D=0.11$ ; then this force increases with tunnelling progress post the structure, and reaches about  $600\text{kN}$  at end of tunnelling ( $z^*/D=6.62$ ). However, the axial force at the head of this is tension with moderate values at  $z^*/D=0.11$  but changes to compression at end of tunnelling. ( $z^*/D=6.62$ ). The response of pile P2, which is the more distant from the tunnel differs from that of P1 as can be seen from Fig. 15(b). The additional axial load in P2 at both construction stages is compressive along the pile full length and has its peak within the pile middle half. Besides,

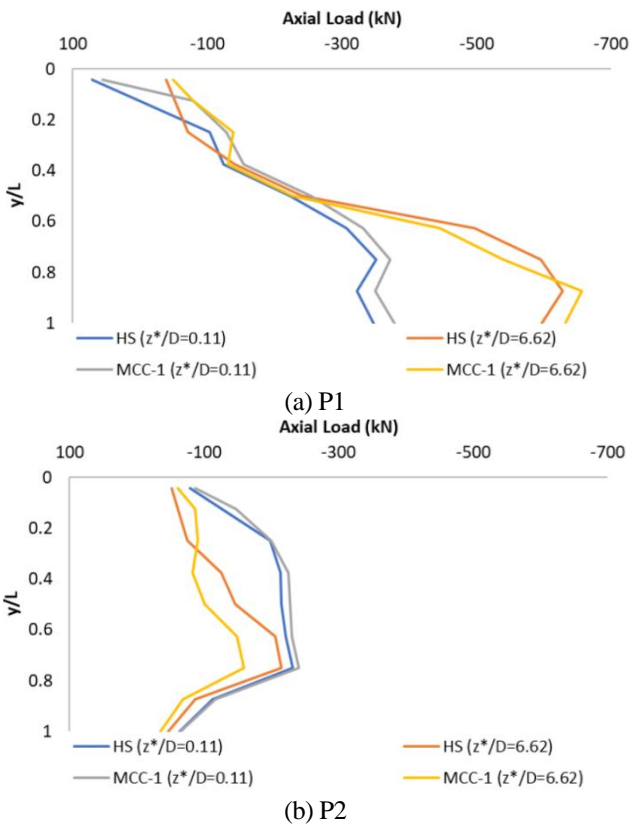


Fig. 15 Pile axial load distribution due to tunneling at time of tunneling crossing under structure ( $z^*/D=0.11$ ) and at end of tunneling ( $z^*/D=6.62$ )

Table 4 Maximum steady state bending moment ( $M_{max}$ ) and normal force ( $N_{max}$ ) in tunnel lining for various soil models

Model type	HS	MC-1	MC-2	MC-3	MC-4	MMC-1	MMC-2
$M_{max}$ (kN.m/m)	45	77.3	83	63	69	50	50.7
$N_{max}$ (kN/m)	609	648.6	656	642	650	607	608

contrarily to P1, the compressive load in P2 decreases with tunnelling progress post the structure. The compressive axial forces induced in piles due to tunnelling results from soil volumes that hang onto the piles after partially losing their support when the underneath soil is removed with tunnelling process. It worth noting that the developed pile axial loads are quiet significant in comparison to the piles axial capacity and the actual "initial" loads existing in piles prior to tunnelling. In the presented example, the initial axial load sustained by one pile was 91 kN at the pile head and 73 kN at the tip (i.e., about 20% of the initial load is carried by skin friction while about 80% is resisted by end bearing).

## 7. Effect of soil modelling on tunnel internal forces

Fig. 16 presents the distributions of the steady-state bending moment and normal force in tunnel lining obtained using the HS model. Results of all other soil models were qualitatively similar to those shown in Fig. 16. Thus, Table 4 compares values of the maximum bending moment and axial force induced in tunnel lining for the different soil material models described in table 2. The maximum values of bending moment and normal force obtained by the various MC models (MC-1 to Mc-4) are about (40% to 84%) and (5% to 8%), respectively, larger than the HS model results. Nonetheless, the maximum values of bending moment obtained by the MMC-1 and MMC-2 models are about 11% to 13% larger than the HS model results, while the predictions of normal force by these proposed methods differ from those calculated using the HS model by less than 1%. It is, therefore, clear that the proposed hybrid models give lining internal forces that are in good agreement with their corresponding HS results, while the MC models fail again to give sufficiently accurate results particularly for the lining bending moments.

## 8. Conclusions

An extensive three-dimensional numerical study is conducted to evaluate the effects of soil material modelling on the structural analysis of tunnelling in soft soils adjacent to piled structures. Seven soil material models are investigated: the reasonable hardening soil model (HS) which is considered as the reference case; four approximate Mohr Coulomb models (MC-1 to MC-4); and two proposed hybrid models (MMC-1 and MMC-2) in which the hardening soil constitutive relation is used for soil at the local, highly-strained zones while the Mohr Coulomb criterion is utilized elsewhere. The assessed results include ground surface and pile cap movements, pile deformation, and tunnel lining internal forces. Based on the analysis of output results for the investigated cases, the following

remarks are drawn.

- The selection of soil constitutive relation has an important effect on the results of three-dimensional tunnel-soil-pile-structure interaction analysis. Noticeable changes among analysis results of different soil models are found in soil deformation, pile cap settlement, pile response, and tunnel lining internal forces. However, the amount of change varies with the analysis parameter of interest.

- All models based on Mohr Coulomb alone failed to produce acceptable results for both system deformation and internal forces and showed differences of up to 80% from the reference HS model results. There are two exceptions: the tunnel lining normal forces differed from the HS model estimates by up to 8% only; and the errors in pile response exceeded 100%.

- The Mohr Coulomb models were also unable to produce some of the system response features. In particular, these models could not produce the sudden reduction in the settlement profile at ground surface that occurred at the pile cap outer edge.

- The various results obtained using the proposed hybrid models are practically reasonable as they differ from the reference HS model results by less than 13% and 20% for system deformation and internal forces, respectively.

- Thus, the proposed hybrid model, which is a compromise between complex and simple solutions, could be of importance to practice engineers as it: (1) decreases computational time (by 27% in the case study problem); and (2) reduces the cost of soil testing (by determining the MC parameters only in the less-strained zones).

## References

- Addenbrooke, T.I. (1996), "Numerical analysis of tunnelling in stiff clay", Ph.D. Dissertation, University of London, London, England.
- Ardakani, A., Bayat, M. and Javanmard, M. (2014), "Numerical modeling of soil nail walls considering Mohr Coulomb, hardening soil and hardening soil with small-strain stiffness effect models", *Geomech. Eng.*, **6**(4), 391-401
- Augarde, C.E., Burd, H.J. and Houlsby, G.T. (1995), "A three-dimensional finite element model of tunnelling", *Proceedings of the 4th Symposium on Numerical Models in Geomechanics- NUMOG V*, Davos, Switzerland, September.
- Brinkgreve, R.B.J. and Vermeer, P.A. (2001), *Plaxis 3D Tunnel Program*.
- Chen, L.T., Poulos, H.G. and Loganathan, N. (1999), "Pile responses caused by tunnelling", *J. Geotech. Geoenviron. Eng.*, **125**(3), 207-215.
- Chen, L.T., Poulos, H.G. and Loganathan, N. (2000), "Approximate design charts for piles adjacent to tunneling operations", *Proceedings of the, GeoEng2000, International Conference on Geotechnical and Geological Engineering*, Melbourne, Australia, November.
- Cheng, C.Y., Dasari, G.R., Chow, Y.K. and Leung, C.F. (2007), "Finite element analysis of tunnel-soil-pile interaction using displacement controlled model", *Tunn. Undergr. Sp. Technol.*, **22**(4), 450-466.
- Clough, G.W. and Leca, E. (1989), *With Focus on the Use of Finite Element Methods for Soft Ground Tunnelling*, in *Tunnels et Micro-Tunnels en Terrain Meuble-du Chantier a la Theorme*, Press de L'Ecole National des Pot et Chaussees, Paris, France, 531-573.

- Dong, W. and Anagnostou, G. (2013), "Calibration of a modified hardening soil model for kakiritic rocks", *Proceedings of the 18th International Conference on Soil Mechanics and Geotechnical Engineering*, Paris, France, September.
- Kahlström, M. (2013), "Plaxis 2D comparison of Mohr-Coulomb and soft soil material models", M.Sc. Dissertation, Luleå University of Technology, Luleå, Sweden.
- Katzenbach, R. and Breth, H. (1981), "Nonlinear 3D analysis for NATM in Frankfurt clay", *Proceedings of the 10th International Conference on Soil Mechanics and Foundation Engineering*, Stockholm, Sweden, June.
- Lee, K.M., Rowe, R.K. and Lo, K.Y. (1992), "Subsidence owing to tunnelling I: Estimating the gap parameter", *Can. Geotech. J.*, **29**(6), 929-940.
- Lee, C.J. (2013), "Numerical analysis of pile response to open face tunnelling in stiff clay", *Comput. Geotech.*, **51**, 116-127.
- Lee, G.T.K. and Ng, C.W.W. (2005), "Three-dimensional numerical simulation of tunnelling effects on an existing pile", *Proceedings of the 5th International Symposium on Geotechnical Aspects of Underground Construction in Soft Ground*, CRC Press, Amsterdam, The Netherlands, June.
- Lee, C.J. and Chiang, K.H. (2007), "Responses of single piles to tunnelling-induced soil movements in sandy ground", *Can. Geotech. J.*, **44**(10), 1224-1241.
- Lee, S.W., Cheang, W., Swolfs, W. and Brinkgreve, R. (2009), "Plaxis-GiD modelling of tunnel-pile interaction", *Proceedings of the 2nd International Conference on Computational Methods in Tunnelling*, Bochum, Germany, September.
- Loganathan, N. and Poulos, H.G. (1998), "Analytical prediction for tunnelling-induced ground movements in clays", *J. Geotech. Geoenviron. Eng.*, **124**(9), 846-856.
- Loganathan, N., Poulos, H.G. and Stewart, D.P. (2000), "Centrifuge model testing of tunnelling induced ground and pile deformations", *Géotechnique*, **50**(3), 283-294.
- Loganathan, N., Poulos, H.G. and Xu, K.J. (2001), "Ground and pile-group responses due to tunnelling", *Soil. Found.*, **41**(1), 57-67.
- Mica, L., Racansky, V. and Krasny, O. (2009), "Analysis of interaction of retaining walls with underground structures in clay", *Proceedings of the 2nd International Conference on Computational Methods in Tunnelling*, Bochum, Germany, September.
- Mohammadi, M. and Tavakoli, H. (2015), "Comparing the generalized Hoek-Brown and Mohr-Coulomb failure criteria for stress analysis on the rocks failure plane", *Geomech. Eng.*, **9**(1), 115-124.
- Moradi, G. and Abbasnejad, A. (2015), "Experimental and numerical investigation of arching effect in sand using modified Mohr Coulomb", *Geomech. Eng.*, **8**(6), 829-844
- Mroueh, H. and Shahrouh, I. (2002), "Three-dimensional finite element analysis of the interaction between tunnelling and pile foundation", *J. Numer. Anal. Meth. Geomech.*, **26**(3), 217-230.
- Mu, L., Huang, M. and Finno, R.J. (2012), "Tunnelling effects on lateral behaviour of pile rafts in layered soil", *Tunn. Undergr. Sp. Technol.*, **28**, 192-201.
- Ng, C.W.W., Lu, H. and Peng, S.Y. (2013), "Three-dimensional centrifuge modelling of the effects of twin tunnelling on an existing pile", *Tunn. Undergr. Sp. Technol.*, **35**, 189-199.
- Pang, C.H., Yong, K.Y., Chow, Y.K. and Wang, J. (2005), "The response of pile foundations subjected to shield tunneling", *Proceedings of the International Symposium on Geotechnical Aspects of Underground Construction in Soft Ground*, Amsterdam, The Netherlands, June.
- Pang, C.H. (2006), "The effects of tunnel construction on nearby piled foundation", Ph.D. Dissertation, National University of Singapore, Singapore.
- PLAXIS (2001), *PLAXIS 3D Tunnel Validation and Verification Manual*, PLAXIS BV & Delft University, Delft, The Netherlands.
- Poulos, H.G. (1979), "Settlement of single piles in nonhomogeneous soil", *J. Geotech. Eng.*, **105**(GT5), 627-641.
- Vahdatirad, M.J., Ghodrat, H., Firouzian, S. and Barari, A. (2010), "Analysis of an underground structure settlement risk due to tunneling-A case study from Tabriz, Iran", *Songklanakarinn J. Sci. Technol.*, **32**(2), 145-152.
- Vergheese, S.J., Nguyen, C.T. and Bui, H.H. (2013), "Evaluation of plasticity-based soil constitutive models in simulation of braced excavation", *J. Geomate*, **5**(2), 672-677
- Xiang, Y., He, S., Cui, Z. and Ma, S. (2005), "A subsurface "drift and pile" protection scheme for the construction of a shallow metro tunnel", *Tunn. Undergr. Sp. Technol.*, **20**(1), 1-5.
- Yang, M., Sun, Q., Li, W.C. and Ma, K. (2011), "Three-dimensional finite element analysis on effects of tunnel construction on nearby pile foundation", *J. Central South Univ. Technol.*, **18**(3), 909-916.
- Zidan, A.F. and Ramadan, O. (2015), "Three dimensional numerical analysis of the effects of tunnelling near piled structures", *KSCE J. Civ. Eng.*, **19**(4), 917-928.
- Zidan, A.F. and Ramadan, O. (2016), "Tunnelling beneath piled structures based on Mohr-Coulomb criterion", *Proceedings of the 4<sup>th</sup> International Conference on Advances in Civil, Structural and Construction Engineering*, Rome, Italy, August.
- Zidan A.F. (2012), "Numerical study of behaviour of circular footing on geogrid-reinforced sand under static and dynamic loading", *Geotech. Geol. Eng.*, **30**(1), 499-510.

CC